Advances in Science and Technology Research Journal

Advances in Science and Technology Research Journal, 2026, 20(6), 78–92
https://doi.org/10.12913/22998624/216736
ISSN 2299-8624, License CC-BY 4.0

Received: 2025.11.05
Accepted: 2026.04.15
Published: 2026.05.01

A computational fluid dynamics based study of the thermal hydraulic performance of shell and tube heat exchanger integrated with metal foam

Rana Qassim Faraj [1*], Abbas J. Jubear Al-jassani[1], Hussein Razzaq Al-Bugharbee[1]

[1] Department of Mechanical Engineering, College of Engineering, University of Wasit, Al-Kut, Wasit, Iraq
* Corresponding author's e-mail: ranaf527@uowasit.edu.iq

ABSTRACT

Improving the thermal-hydraulic performance of shell and tube heat exchangers (STHX) is a critical objective in modern engineering to reduce the energy consumption and operational costs while ensuring reliable performance. This study utilises numerical simulation (ANSYS Fluent 2025 R2) to evaluate the performance of STHX using six copper metal foam baffles, compared to a conventional design featuring solid baffles. The study analyses various baffle cut-off ratios (20%, 30%, 40%, and 50%) and thicknesses (2, 6, 10, 14, and 18 mm) across a range of fluid flow rates from 1.2 to 2 kg/s. The results demonstrate that the metal foam baffles reduce system pressure loss by up to 28% compared to solid baffles while simultaneously enhancing heat transfer. The optimum thermal performance factor (TPF) of 2.138 was achieved at a 20% cut-off ratio and a mass flow rate of 1.2 kg/s, resulting in a 48.4% enhancement in the Nusselt number (Nu) compared to the solid baffle arrangement. Moreover, augmenting the baffle thickness to 18 mm resulted in an enhanced TPF of 2.465 at the minimum mass flow rate of 1.2 kg/s. This arrangement enhanced the Nusselt number by 55.8% and reduced the pressure drop by 25.5% compared to similar solid baffles. These results validate that copper foam baffles are an exceptionally effective approach for improving the overall efficiency of STHXs.

Keywords: STHX, thermal hydraulic performance, metallic foam baffles, numerical simulation.

INTRODUCTION

The STHX is a prevalent and extensively utilised type in industrial applications, power plants, and cooling systems, due to its significant efficacy in heat transfer and adaptable design, which accommodates high pressures and temperatures. The configuration of STHX involves one fluid traversing a collection of parallel tubes, while a second fluid, either in liquid or gaseous form, circulates around the external surface of these tubes within a cylindrical casing. This configuration facilitates effective heat transfer between the fluids, rendering STHX a flexible option [1, 2]. Research has concentrated on enhancing the efficiency of STHX on both the tube and shell sides. The exchanger, including segmental baffles, is the most prevalent owing to its straightforward design, economical nature, and superior heat transfer efficiency attributed to its cross-flow characteristics [3].

Numerous applications in heat management, thermal energy storage, heat sinks, and heat exchangers utilize metal foams, which are effective materials for enhancing heat transfer. Aluminum and copper foams have proven to be reliable materials when used in various types of heat exchangers, with no significant issues related to clogging or damage from debris [4]. Hossein et al. [5] evaluated the performance STHX when fully or partially filled with porous foam, comparing them with a conventional foam-free design. The study relied on numerical simulations using (CFD) techniques to analyse the temperature distribution and pressure drop. The results showed that the use of porous foam significantly

enhanced thermal performance, with thermal efficiency increasing by up to 60% compared to the conventional design. However, a larger pressure drop was observed. Partial foam filling reduced the pressure loss to approximately half that of complete filling.

An experimental study on a vertical cylinder under a constant heat flux and fitted with porous aluminum fins was achieved by Kiwan et al. [6]. The variables examined were cylinder diameters (50, 60, and 80 mm), quantities of fins (1, 3, and 5), thicknesses (10 and 20 mm), and types of porous material. The results indicated that the highest increase in heat transfer coefficient (131.8%) was recorded when a 50 mm diameter cylinder was fully fitted with type A fins compared to a fin less cylinder.

The heat transfer and fluid flow behavior in a three-dimensional cylindrical heat exchanger containing porous filling was studied by Rong et al. [7]. The axisymmetric Lattice Boltzmann Method (LBM) thermal model was used to investigate the effect of geometric and physical variables (block width, block height, block spacing, Darcy number Da, and porosity (ε) on the flow characteristics and temperature fields. The results showed that the (Nu) increases as the height of the porous blocks increases, while it decreases with increasing width. Increasing the block spacing reduces heat mixing and lowers Nu. Decreasing Da (decrease in permeability) leads to an increase in Nu due to enhanced flow near the tube wall, while the effect of porosity is relatively slight compared to other parameters. Chen et al. [8] evaluated the thermal-hydraulic performance of a STHX within a waste heat recovery system. The study compared units with copper foam baffles against those with no baffles or solid baffles. The research utilized six baffles, systematically positioned with pore densities varying between 5 and 40 PPI. The results indicated that the most significant enhancement in thermal performance was achieved at 40 PPI, surpassing both baffle-free and solid baffle exchangers.

Alhusseny et al. [9] investigated the performance of double-tube heat exchangers using a composite technique that enhances heat transfer by integrating a porous layer and a rotating metal foam. The results indicated that incorporating metal foam enhanced thermal efficiency relative to traditional designs, with the higher-density foam (30 PPI) demonstrating superior thermal performance but necessitating a larger pumping capacity. The composite design also demonstrated its ability to reduce pumping energy consumption, with the highest efficiency recorded at a rotation speed of 500 rpm and a thermal improvement ranging from 200% to 300%. Hu et al. [10] investigated the heat transfer and pressure drop of humid air passing through a copper foam treated with a hydrophobic coating under dehumidification conditions. Foams of various PPI (i.e.5 and 40) were utilised, and the influences of temperature, humidity, air velocity, and cooling water temperature were examined. The findings showed that the hydrophobic coating improved the heat transfer coefficient by 5–34%, especially at low humidity levels (30–50%) and a density of 20 PPI, while simultaneously increasing pressure loss by up to 95% at elevated humidity. Complementing this, Dongellini et al. [11] assessed the thermal and hydraulic performance of air-to-water heat exchangers constructed from high-porosity aluminum foam (>96%, 10 PPI) and contrasted them with traditional finned exchangers. Several techniques for affixing the foam to the copper tubes were examined, including compression fitting, thermal grease, and epoxy bonding. The results indicated that epoxy bonding enhanced heat transport by as much as 110% and achieved optimal equilibrium between thermal and hydraulic performance. However, the pressure drops increased by 13–42% relative to traditional finned exchangers, which can limit airflow in air conditioning systems.

The thermal performance of a STHX for thermal energy storage using a combination of metal foam and longitudinal fins was analyzed by Yang et al. [12] through a numerical model. The study included four configurations: a conventional system (PCM only), a system with fins (Fin-PCM), a system containing metal foam (Foam-PCM), and a hybrid system combining both (Fin-Foam-PCM). Aluminum foam with a porosity of 96% and a density of 10 PPI was used, bonded to copper tubes in two ways: S-type (sandwich packaging) and K-type (kebab packaging). The findings indicated that the hybrid system (Fin-Foam-PCM) surpassed the conventional system, enhancing treatment time by 90.5%. The metal foam, on the other hand, improved heat transfer by 82.1% while increasing flow resistance by 35%. In contrast, the fins relatively improved performance by only 42.7%. Tamkhade et al. [13] analyzed the thermal and hydraulic performance of heat exchangers and numerically optimized them using ANSYS

Fluent software. A tube-in-tube heat exchanger was used, with the annular space between the two tubes filled with nickel metal foam, having a porosity of 0.9 and a pore density ranging from 10 to 50 PPI. The findings demonstrated that the 50 PPI metal foam had a significantly better thermal performance, showing an 85% increase in the heat transfer coefficient, which greatly surpassing the 25% improvement seen with the 10 PPI foam. In contrast, the pressure loss increased by 18% at 10 PPI and reached 92% at 50 PPI due to the increased hydraulic resistance to flow. The thermal and hydraulic performance of a fan coil heat exchanger with 52 tubes organized in four rows and covered with copper foam in place of traditional fins was examined by Hassan et al. [14] using COMSOL software. The influence of air velocity (1–10 m/s) and porosity (0.88–0.98) on thermal and hydraulic performance was examined. The results showed that the heat transfer coefficient increased from 4.11 to 141.1 W/m²•K with increasing air velocity. The pressure loss escalated from 19.03 Pa to 335.76 Pa within the identical velocity range. Optimal system performance was observed under conditions of moderate porosity (0.93) and medium-range air velocities (3–5 m/s).

Tian et al. [15] assessed the efficacy of STHX in diesel engine exhaust heat recovery systems by replacing conventional baffles and fins with metal foam substitutes. The numerical analysis employed the Darcy-Forchheimer-Brinkman equations and the LTNE model. The findings indicated that the foam baffles and fins enhanced heat transmission by 92.14%, reduced pressure loss by 64.7%, and lowered weight by 11.35% compared to the conventional design. The effect of using copper foam baffles inside double-pipe heat exchangers on thermal and hydraulic performance was studied using numerical simulations and experimental measurements by Zuhair et al. [16]. ANSYS Fluent 2020 R2 was used for numerical simulations, analyzing the effects of several design and operational parameters, including baffle angle (β = 0°, 60°, 120°, 180°), pore density (PPI = 10–50), baffle thickness (10, 20, 30 mm), and flow rates (2–6 L/min). The results showed that the best overall performance criterion (PEC) was achieved at PPI = 40, β = 180°, thickness = 10 mm, and flow = 3 L/min.

Jubear et al. [17] assessed a double pipe heat exchanger using metal foam and nanofluids with a CFD-based numerical model. The results showed that the metal foam improved the heat transfer coefficient by 45–70%, the nanofluids by 25–40%, and the combination of the two improved the Nusselt number by 90–120% compared to a conventional exchanger, with a 60–95% increase in pressure loss. Jadhav et al. [18] studied the impact of graded metal foams on the thermal and hydraulic performance of a straight tube heat exchanger (1 × 0.10 m). The researchers utilized high-porosity aluminum foam (with porosity ε = 0.90) at two densities (20 and 45 PPI) and also tested composite foams made of copper and aluminum. A numerical analysis was conducted using ANSYS Fluent 19.2, employing DEF, LTNE, and k-ω models. The results showed that the negative gradient configuration (using 45 PPI and 20 PPI foam) enhanced heat transfer by 8.7% to 32.3% and significantly decreased pressure loss by up to 84% compared to an empty tube. Copper foam enhanced the Nusselt number by 1% at a higher expense.

This study presents a novel research perspective that departs from previous studies on the utilization of metal foams to enhance heat exchanger performance. Traditional baffles in STHX involve a fundamental compromise: enhanced heat transfer versus elevated pressure drop. Metal foams, as continuous porous materials, present a transformative alternative by providing an enhanced surface area and uniform mixing. A critical knowledge gap remains in understanding the coupled effects of essential parameters: baffle cut ratio, foam thickness, and mass flow rate.

Therefore, a numerical study is needed to elucidate the interrelationship between these factors and determine the optimal baffle configuration for optimal thermal-hydraulic performance. Our methodical analysis seeks to clarify this complex relationship. It provides an innovative design framework that surpasses traditional compromises and promotes the advancement of next-generation, high-efficiency heat exchangers.

NUMERICAL SIMULATION

To numerically characterise technical challenges, a set of partial differential equations must be solved using specialized numerical methods. The finite volume approach is the most suitable option for addressing the continuity, momentum, and energy equations, using ANSYS 2025 R2. The SIMPLE scheme was used to couple the pressure and velocity fields.

The equations for pressure, momentum, energy, kinetic energy, and turbulence dissipation rate were discretised using second-order upwind schemes to ensure precise results. Convergence criteria were set to 10^{-4}, 10^{-4}, 10^{-7}, and 10^{-4} for the continuity, momentum, energy, and turbulence equations, respectively. Under-relaxation factors of 0.3 for pressure, 0.7 for momentum, and 1.0 for energy were established, which facilitated the stability and rapid convergence of the numerical solution.

The present study relied on the geometric dimensions of a STHX previously presented by Nie et al. [19], which was also used for numerical validation. The model consists of a 143 mm diameter, 600 mm long shell, containing 13 tubes with an outer diameter of 22 mm arranged in a triangular layout at an angle of 60°, with six solid baffles as shown in Figure 1. To improve performance, the heat exchanger was equipped with an open cell copper foam with a porosity of 0.9 and a pore density of 40 PPI, comparable to conventional solid baffles. The effect of varying cut ratios (BCs): 20%, 30%, 40%, and 50% in the opposite direction, distributed evenly within the shell was also considered in the analysis. The influence of foam baffle thickness (S) was also examined, considering thickness values of 2, 6, 10, 14, and 18 mm, and their performance was studied at different flow rates of 1.2, 1.4, 1.6, 1.8, and 2.0 kg/s. The thermophysical properties of the materials which was using listed in Table 1. Forty simulations were conducted to derive the optimal STHX design in terms of balancing thermal and hydraulic performance.

Mathematical assumptions

A set of basic simplifications was adopted, as follows:

1. Neglecting the influence of leakage that may occur through the baffles-shell inner surface zones.
2. Considering the turbulence condition flow for the flow between the shell and the tubes, while a local laminar condition was considered for the flow through the metal foam zone. This is justified by the great flow resistance and low velocity of flow through the foam.
3. Applying a local thermal nonequilibrium (LTNE) model to represent the interaction in the zone between water and the metal foam skeleton. In addition, the metal foam was proposed to be homogeneous and isotropic.
4. Proposing the consistency of the thermophysical properties of both water and the metal foam and their independency of temperature.

Governing equation

Governing equations are used to analyze fluid flow coupled with heat transfer. The Navier Stokes equations describe the water flow field in a fluid region, while the flow field within a homogeneous, isotropic porous medium is represented by momentum equation, which is derived from the extended Brinkmann–Forchheimer Darcy model. Governing Equations 1–7 include:

- Mass conservation (continuity equation):

This equation states that the mass of any closed system remains constant and does not change with time, in accordance with the principle of mass conservation [23].

$$\frac{\partial \mathrm{u}}{\partial \mathrm{x}} + \frac{\partial \mathrm{v}}{\partial \mathrm{y}} + \frac{\partial \mathrm{w}}{\partial \mathrm{z}} = 0 \tag{1}$$

- Momentum equations:

The rate of change of momentum is equal to the net force acting on the body according to the Navier-Stokes equations and Newton's second law of motion [24]:

- X-axis

$$\left(\mathrm{u}\frac{\partial \mathrm{u}}{\partial \mathrm{x}} + \mathrm{v}\frac{\partial \mathrm{u}}{\partial \mathrm{y}} + \mathrm{w}\frac{\partial \mathrm{u}}{\partial \mathrm{z}} = \right.$$
$$= -\frac{\partial \mathrm{p}}{\partial \mathrm{x}} + \frac{1}{\varepsilon Re}\left(\left(\frac{\partial^2 \mathrm{u}}{\partial x^2} + \frac{\partial^2 \mathrm{u}}{\partial y^2} + \frac{\partial^2 \mathrm{u}}{\partial z^2}\right)\right) - \tag{2}$$
$$-\frac{1}{Da\ Re}\mathrm{u} - \frac{\mathrm{F}}{\sqrt{Da}}u|\vec{\mathrm{U}}|\ \frac{1}{\varepsilon^2}$$

Table 1. The thermophysical properties of materials [20, 21,22, 23]

Physical properties	Water	Copper	Steel
Density (kg/m^3)	998.2	8978	8030
Thermal conductivity (W/m. k)	0.6	387.6	16.27
Specific heat (J/kg. k)	4182	381	502.48
Dynamic viscosity (kg/m. s)	0.001	-	-

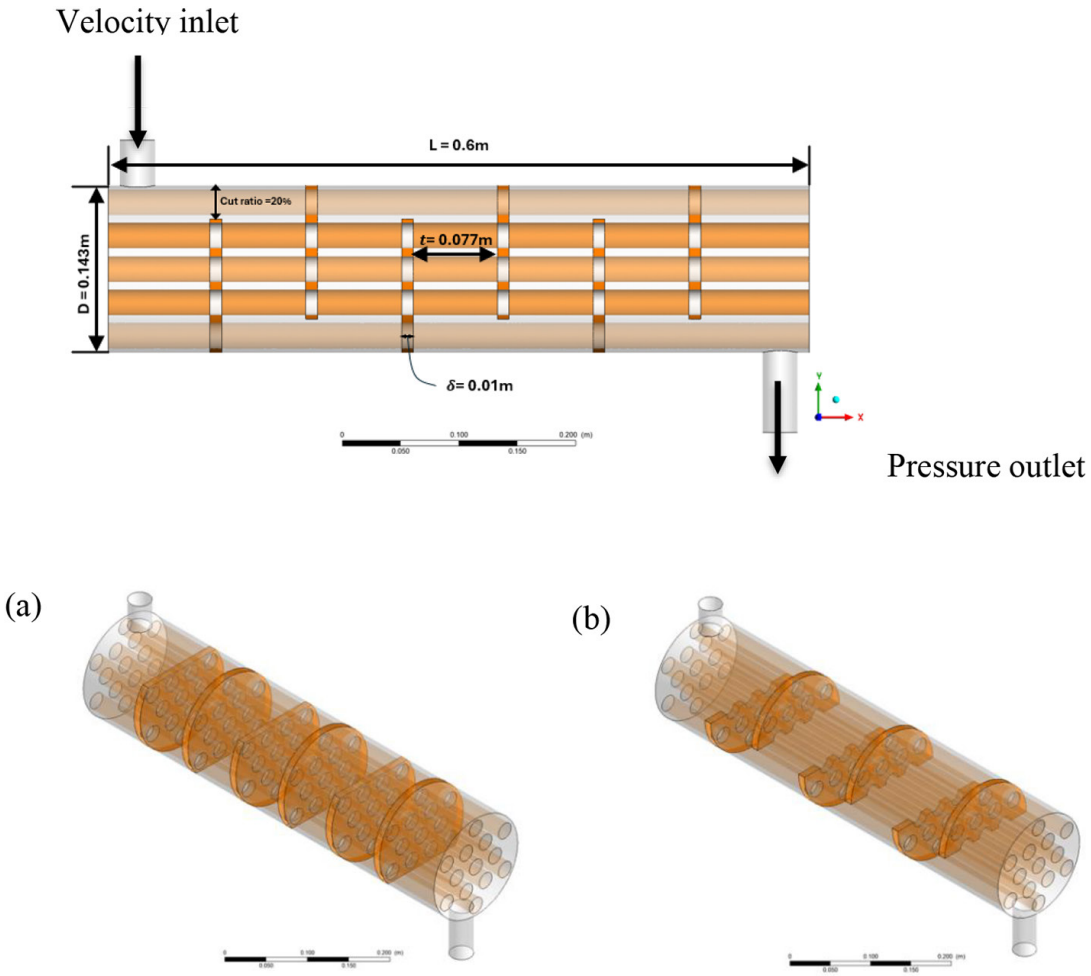

Figure 1. Geometry of physical model with various baffle cut ratios (a) 20% (b) 50%

- Y-axis

$$\frac{1}{\varepsilon^2}\left(u\frac{\partial \mathrm{v}}{\partial \mathrm{x}} + \mathrm{v}\frac{\partial \mathrm{v}}{\partial \mathrm{y}} + \mathrm{w}\frac{\partial \mathrm{v}}{\partial \mathrm{z}}\right) = -\frac{\partial \mathrm{p}}{\partial \mathrm{y}} + \frac{1}{\varepsilon Re}\left(\left(\frac{\partial^2 \mathrm{v}}{\partial x^2} + \frac{\partial^2 \mathrm{v}}{\partial y^2} + \frac{\partial^2 \mathrm{v}}{\partial z^2}\right)\right) - \frac{1}{Da\,Re}\mathrm{v} - \frac{\mathrm{F}}{\sqrt{Da}}\mathrm{v}\,|\vec{\mathrm{U}}| \quad (3)$$

- Z-axis

$$\frac{1}{\varepsilon^2}\left(u\frac{\partial \mathrm{w}}{\partial \mathrm{x}} + \mathrm{v}\frac{\partial \mathrm{w}}{\partial \mathrm{y}} + \mathrm{w}\frac{\partial \mathrm{w}}{\partial \mathrm{z}}\right) = -\frac{\partial \mathrm{p}}{\partial \mathrm{z}} + \frac{1}{\varepsilon Re}\left(\left(\frac{\partial^2 \mathrm{w}}{\partial x^2} + \frac{\partial^2 \mathrm{w}}{\partial y^2} + \frac{\partial^2 \mathrm{w}}{\partial z^2}\right)\right) - \frac{1}{Da\,Re}\mathrm{w} - \frac{\mathrm{F}}{\sqrt{Da}}\mathrm{w}\,|\vec{\mathrm{U}}| \quad (4)$$

- Energy equations:

The fluid energy equation in a porous medium (LTNE) is given by

$$\left(u\frac{\partial T_f}{\partial \mathrm{x}} + \mathrm{v}\frac{\partial T_f}{\partial \mathrm{y}} + \mathrm{w}\frac{\partial T_f}{\partial \mathrm{z}} = \frac{1+K_f}{Pr\,Re}\left(\left(\frac{\partial^2 T_f}{\partial y^2} + \frac{\partial^2 T_f}{\partial z^2}\right)\right) + \frac{h_{sf}\,a_{sf}}{K_{sf} PrRe}\left(T_s - T_f\right)\right. \quad (5)$$

- Energy equation of the solid matrix (LTNE) is

$$0 = \frac{\partial^2 T_f}{\partial y^2} + \frac{\partial^2 T_f}{\partial z^2} + \frac{h_{sf}\,a_{sf}}{K_{se}}\left(T_f - T_s\right) \quad (6)$$

The energy equation for an incompressible fluid can be represented as a heat equation describing the static temperature, in the absence of foam as:

$$(\mathrm{u}.\,\nabla)\,\mathrm{T} = \alpha\nabla.\,(\nabla \mathrm{T}) \quad (7)$$

Mesh independency

During the meshing process, the tetrahedral elements were selected and utilized to discretize the geometry models using Ansys Fluent as shown in Figure 2. To accurately represent the steep gradients in both temperature and velocity near the tube surface, a boundary layer mesh was generated around the surface. To evaluate the effect of the mesh on the simulation results, six mesh systems with element numbers of 2,611,524, 3,071,218, 3,430,912, 3,890,606, 4,150,300, and 4,409,994 were tested for a shell and tube heat exchanger (STHX) equipped with six copper foam baffles 20% cut ratio at a flow rate of 1.2 kg/s. Figure 3 shows the change in both pressure drop and the outlet water temperature calculated using these mesh systems. The relative errors of the pressure drop and outlet temperature at mesh numbers 3,890,606, 4,150,300 were 0.08% and 0.06% respectively. Therefore, the mesh with 3,890,606 elements was adopted in the current study to ensure sufficient accuracy while reducing numerical cost.

Boundary and initial conditions

As mentioned earlier, the LTNE model was utilized to model the flow working fluid through the metal foam, in the case of highly conductive metallic foams with large surface areas, there is an instantaneous thermal contrast between the liquid and solid phases within the porosity, especially at high flow rates and large heat transfer coefficients [19]. Therefore, the assumption of local thermal equilibrium (LTE) does not accurately reflect the physical behavior within the foam.

The momentum equation in the metal foam was modeled using the Brinkman Forchheimer Darcy model. Accordingly, the velocity coefficients representing the viscous resistance (represented by the inverse of the permeability), the inertia loss coefficient (F), and the interface area (*asf*) were determined, which were calculated according to Equations 8–12. The interface heat transfer coefficient (*h*sf) was determined using the user-defined function (UDF) as a function of velocity [25], as per the ANSYS Fluent User Manual.

$$\frac{K}{dp^2} = 0.00073\,(1-\varepsilon)^{-0.224}\left(\frac{d_f}{dp}\right)^{-1.11} \quad (8)$$

$$\mathrm{F} = 0.00212(1-\varepsilon)^{-0.132}\left(\frac{d_f}{dp}\right)^{-1.36} \quad (9)$$

The interface area of the metal foam is determined based on the following mathematical equation [18,26]

$$a_{sf=}\frac{3\pi d_f\left(1-e^{-\left(\frac{(1-\varepsilon)}{0.04}\right)}\right)}{\left(0.59\,d_p\right)^2} \quad (10)$$

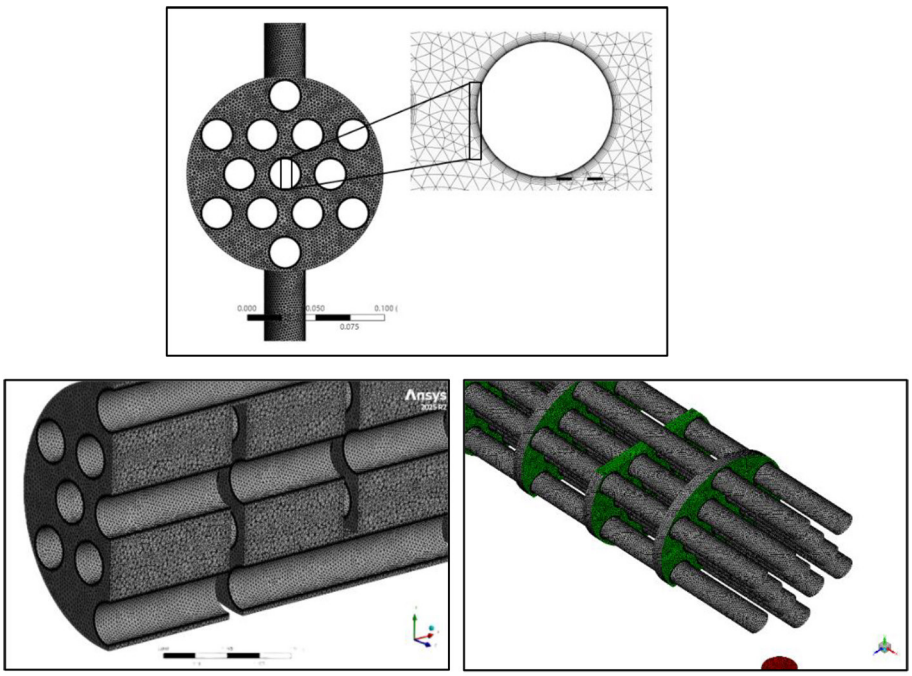

Figure 2. STHX grid system with segmental baffle

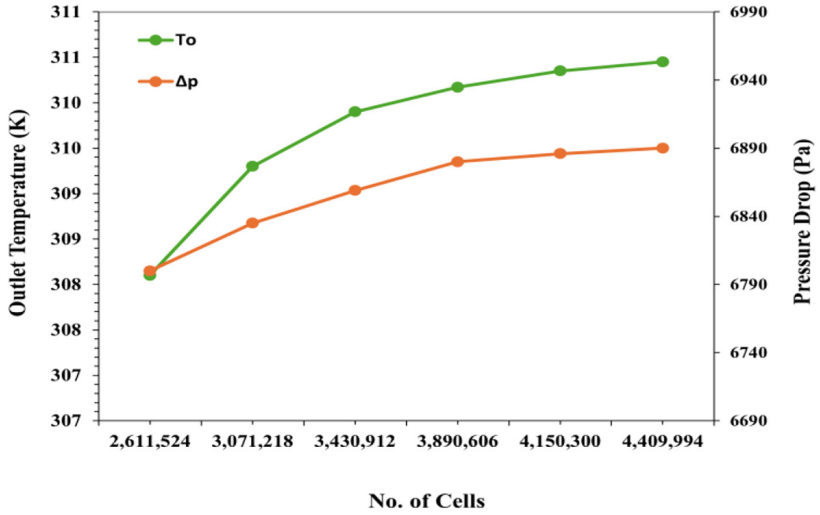

Figure 3. Study of the mesh independence on pressure drop and water temperature at the outlet

In the above equations, ε represents porosity, while d_p and d_f represent the pore size and fiber diameter in the metal foam, respectively

$$Viscous\ resistance = \frac{1}{K} \tag{11}$$

$$Inertial\ resistance = \frac{2F}{K^2} \tag{12}$$

The interfacial heat transfer coefficient h_{sf} between water and the metal foam was estimated using empirical equations developed by Zukauskas [27]

$$\begin{gathered} h_{sf} = 0.76\, Re_d^{0.4} Pr^{0.37} \frac{K_f}{d}, \\ 1 \le Re_d \le 40 \\ h_{sf} = 0.52\, Re_d^{0.5} Pr^{0.37} \frac{K_f}{d}, \\ 40 \le Re_d \le 1000 \\ h_{sf} = 0.26\, Re_d^{0.6} Pr^{0.37} \frac{K_f}{d}, \\ 1000 \le Re_d \le 2000 \end{gathered} \tag{13}$$

The tube walls were considered as constant-temperature boundaries, with:

$$u = v = w = 0, \text{ and } T_{wall} = 325 \text{ K} \tag{14}$$

The surfaces of the shell are treated as adiabatic boundaries, where:

$$\begin{gathered} \text{u = v = w = 0, and the normal} \\ \text{temperature gradient is zero } \frac{\partial T}{\partial n} = 0 \end{gathered} \tag{15}$$

The water outlet surface represents the pressure outlet boundary, where:

$$\left(\frac{\partial u}{\partial x} = \frac{\partial V}{\partial y} = \frac{\partial w}{\partial z} = 0\right) \text{ and } (p_{out} = 0) \tag{16}$$

The initial conditions for the computational domain were set such that the velocities were:

$$\begin{gathered} \text{u = v = w = 0 and} \\ \text{the temperature was } T = 300 \text{ K.} \end{gathered} \tag{17}$$

The symbols u, v, and w represent the velocity components along the x, y, and z axes, respectively.

DATA PROCESSING

The heat transfer coefficient is calculated using equation [21]:

$$H = \frac{Q}{A \cdot \Delta T_m} \quad where$$

$$Q = \frac{M \cdot cp \cdot (Tout - Tin)}{A \cdot \Delta T_m} \tag{18}$$

$$\Delta T_m = \frac{(T_w - T_{in}) - (Tw - T_{out})}{ln\left[\frac{(T_w - T_{in})}{Tw - T_{out}}\right]} \tag{19}$$

The Nusselt number (Nu) is defined by the following equation [28]:

$$Nu = \frac{hD}{k} \tag{20}$$

The hydraulic diameter on the side of shell is defined as follows [28]:

$$D = \frac{1.1}{d_o}\left(Pt^2 - 0.917 {d_o}^2\right) \tag{21}$$

The thermal Performance factor (TPF) standard is used to assess the efficiency STHX from both thermal and hydraulic perspectives [29]:

$$TPF = \frac{(Nu/Nu_o)}{(\Delta P/\Delta P_o)^{\frac{1}{3}}} \quad (22)$$

where: Nu and Nu_o represent the Nusselt number in STHX equipped with foam baffles and solid baffles, respectively. T_{in} and T_{out} represent the inlet and outlet temperatures on the shell side, while T_w represents the tube wall temperature. d_o represents the outer diameter of the tube and pt represents the tube pitch ΔP and ΔP_o represent the pressure drop across the STHX with foam baffles and solid baffles, respectively, while M represents the mass flow rate and c_p represents the specific heat capacity.

RESULTS AND DISCUSSION

Model validation

To test the accuracy of the simulation software (ANSYS 2025 R2), a numerical model of the shell and tube heat exchanger was analysed prior to utilising its dimensions to construct a 3D model of the shell and tube heat exchanger that integrates metal foam (MF) for this investigation. The validation approach was grounded in research by Nie et al. [19], which analysed a system including 36 tubes, each with a diameter of 16 mm. The shell had a diameter of 143 mm and a length of 600 mm. Validation was conducted by examining the fluctuations in pressure drop and heat transfer coefficient on the shell side at flow rates of 0.5, 1, 1.5, and 2 kg/s using a counterflow setup. This resulted in average deviations of 4.25% for pressure drop and 2.8% for the heat transfer coefficient, as illustrated in Figure 4.

Numerical results

Since the characteristics of foam baffles in heat exchangers can be adjusted by varying parameters such as baffle cut ratios, thickness, porosity, and pore density. Consequently, the study examines the impact of these parameters on heat transfer performance. The results, including the outlet water temperature (Tout) and the Nusselt number (Nu), were obtained and analysed across five different flow rates. Furthermore, the hydrodynamic performance, regarding pressure drop (Δp), was examined. The influence of all parameters associated with the foam baffles on heat exchanger performance was assessed, resulting in the identification of the optimal design for these baffles.

The effect of cut ratios for baffle

In this section, the thermal-hydraulic performance of a STHX equipped with solid and metal foam baffles is analysed. The comparison is carried out at various baffle cut ratios while maintaining a constant baffle thickness of S = 10 mm. The pore density (PPI = 40), porosity (0.9), and number of baffles (N = 6) are also maintained constant throughout the study. The outlet water temperature (Tout), Nusselt number (Nu), pressure drop

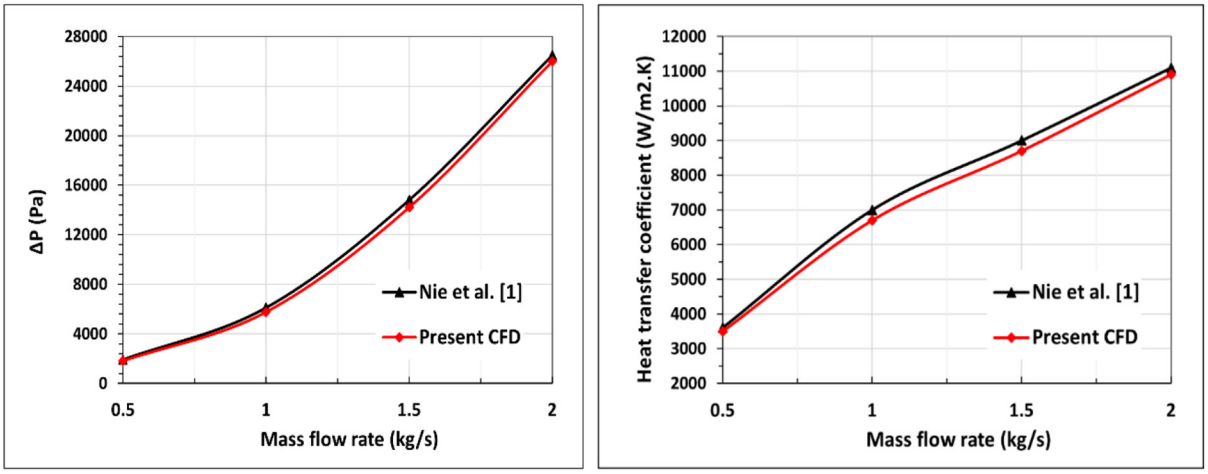

Figure 4. Validation of Nie et al. [19]

(Δp), and thermal performance factor (TPF) for the heat exchanger equipped with solid and foam baffles are illustrated in Figure 5.

The results indicated that a copper foam baffle improved the thermal performance of the heat exchanger due to their large surface area and high thermal conductivity, as shown in Figure 5a. At a flow rate of 1.2 kg/s, the outlet water temperature reached 310.17 K with a baffle cut ratio (Bc) of 20%. In contrast, the temperature of the solid baffles was 305.82 K. Additionally, it was noted that increasing the baffle cut ratio (Bc) resulted in a decrease in the outlet water temperature. Specifically, for baffle cut ratios of 30%, 40%, and 50%, the recorded outlet temperatures were 309.4 K, 308.23 K, and 307.37 K, respectively, at the same flow rate of 1.2 kg/s. This is due to the reduced effective heat transfer area of the foam inserts at higher (Bc), which leads to reduced flow turbulence. The enhancement ratio of the maximum temperature difference is 42% relative to the solid baffle. As the mass flow rate escalates, the exit water temperature progressively diminishes in all scenarios, attributable to the reduced residence time within the heat exchanger.

Figure 5b depicts the relationship between the Nusselt number (Nu) and the mass flow rate (M). It shows that the (MFB-20%) configuration achieves the highest Nu values, with an enhancement ratio of 48.4%. This signifies its superior efficiency in enhancing heat transfer, mostly attributable to heightened turbulence. As the baffle cut ratio increases to 30%, 40%, and 50%, the Nusselt number gradually diminishes due to a reduction in turbulence intensity and the greater open areas diminishing the efficacy of thermal mixing. Conversely, an increase in mass flow rate enhances the Nusselt number (Nu) by raising the effective Reynolds number (Re), which results in a reduction in thermal boundary layer thickness, significantly improving heat transfer by convection.

As demonstrated in Figure 5c, the pressure drop (Δp) is lower when copper foam is used compared to solid baffles across various (Bcs) and flow rates. This decrease in pressure drop occurs because the partial flow through the copper foam reduces both flow deflection and the acceleration needed. Moreover, increasing the (Bc) lowers the overall resistance, which leads to a corresponding decrease in the thermal performance of the STHX. The pressure drop escalates with a rising flow rate in all instances, reaching 31% at 50% Bc and 27% at 20% Bc at 2 kg/s flowrate, attributable to the heightened flow velocity and the corresponding increase in frictional and dynamic losses.

Figure 5d illustrates that the thermal performance factor (TPF) values decrease gradually with an increase in mass flow rate across all baffle cut ratios (Bcs). This reduction is primarily attributed to the increased water velocity, which leads to a greater pressure drop. The improvement in heat transfer does not progress at the same rate, leading to a reduced relative TPF value, which reached 1.804 at a flow of 2 kg/s and a 20% Bc. Nevertheless, the peak TPF values occur at low flow rates; where it was 2.138 at a flow of 1.2 kg/s and a 20% Bc, which is 16% higher than at 2 kg/s flow rates. Under these conditions, the fluid is compelled to pass through or circumvent the baffles, thereby augmenting turbulence and significantly improving heat transfer. In contrast, when the value of (Bc) increases, the TPF values diminish across all flow rates. The reduced flow through the foam baffles results in decreased turbulence from the porous metal, thereby reducing the enhancement of heat transfer, despite the lower pressure drop encountered.

The effect of thickness for baffles

This section analyses the foam thickness (S) influence on the performance of a STHX. Figure 6a illustrates that a thickness of 2 mm yields inferior thermal performance. This arises from inadequate depth, leading to heightened internal conductive resistance and contact resistance, thus diminishing the effective heat exchange surface area. Conversely, the solid baffle produces increased turbulence, hence improving the convection coefficient at an equivalent thickness. The percentage enhancement in temperature difference compared to solid baffles decreased from 48.6% 1.2 kg/s to 43% at 2 kg/s of 18 mm thickness, due to a reduction in residence time. The results indicate that increased thickness enhances heat transfer performance at all flow rates, where increases the enhancing ratio of temperature difference from 29% at 6 mm to 48.6% at 18 mm chiefly due to the augmented heat transfer surface area.

As shown in Figure 6b, the Nusselt number (Nu) rises with a higher mass flow rate. A 55.8% increase was seen at 1.2 kg/s and a baffle thickness of 18 mm compared to the solid baffle. Generally, increasing foam thickness typically results in higher Nu values. This is attributed to a larger effective surface area (A_{eff}), improved internal thermal conductivity (k_{eff}), and enhanced

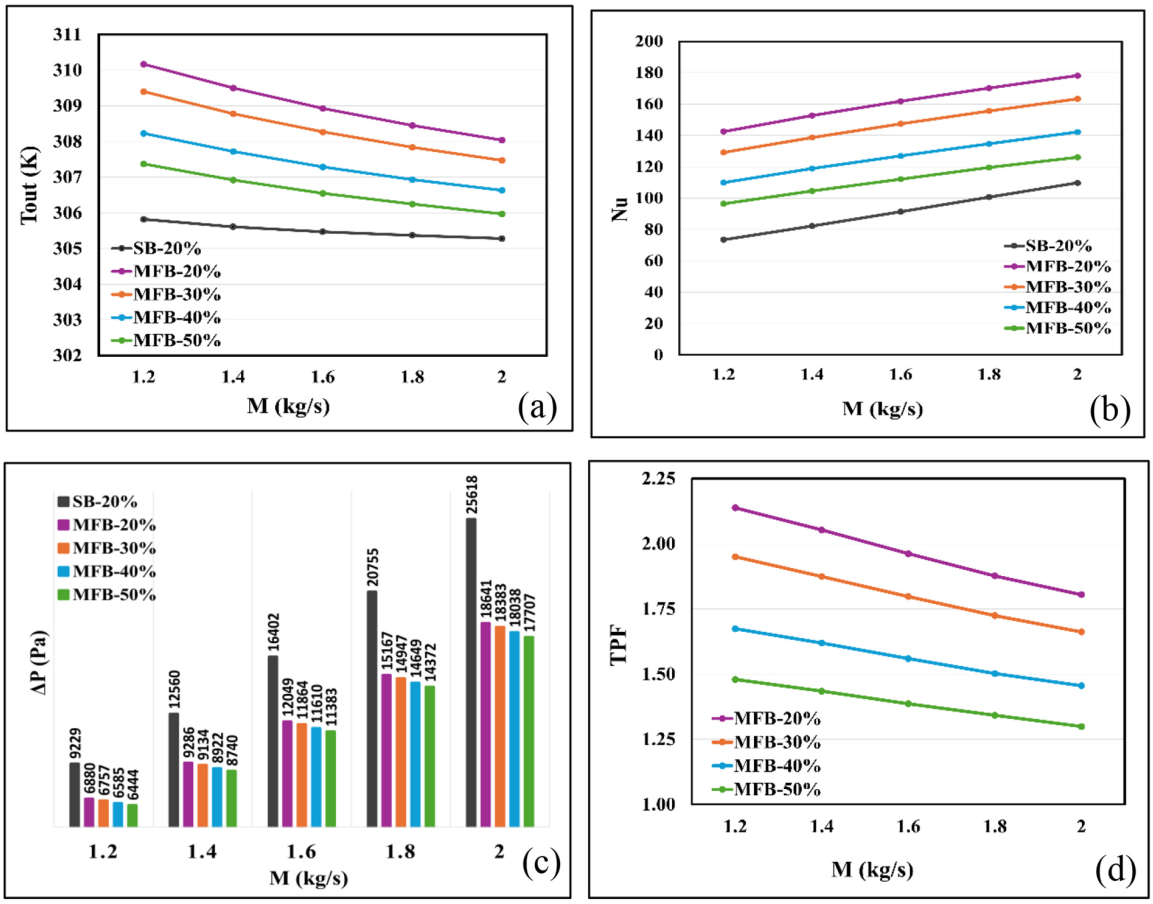

Figure 5. Outlet water temperature, Nu and TPF of STHX with different baffle cut ratios (Bcs) (foam baffles at N = 6 and S = 10 mm PPI=40)

kinetic heat transfer within the pores. However, the increase in Nu corresponds with heightened pressure losses, indicating an optimal thickness that balances thermal and hydraulic performance.

As shown in Figure 6c, the pressure drops increases progressively with the increasing mass flow rate from 1.2 to 2 kg/s, with an increase of approximately 63% from the lowest to the greatest flow rate. At each flow rate, the pressure drop (ΔP) increases with increasing thickness due to the reduction of the open area and the elongation of the flow path. At a mass flow rate of 2 kg/s, ΔP attains approximately 17,538 Pa at a thickness of 2 mm and roughly 19,487 Pa at a thickness of 18 mm, an increase of approximately 10% compared to the lowest thickness. Conversely, for a mass flow rate of 1.2 kg/s, the ΔP values are comparable across all thicknesses, varying from around 6.400 to 7.200 Pa. Therefore, it is clear that the pressure drop in the STHX is predominantly influenced by the mass flow rate and the thickness of the foam layer.

The data presented in Figure 6d show that the thermal performance factor (TPF) increases significantly with the thickness of the metal foam layer across all mass flow rates. This enhancement is due to the increased internal surface area for heat exchange and the improved overall thermal conductivity of the cross-section, which improves convection and conduction heat transfer. A consistent enhancement in the heat transfer coefficient was noted at greater thicknesses (10–18 mm) due to the turbulence induced within the porous structure. At the minimum flow rate of 1.2 kg/s, the 18 mm thickness exhibited superior performance, registering a TPF value of 2.465. The efficacy of augmenting foam thickness in improving heat transfer efficiency, especially at reduced flow rates, is unequivocally evidenced.

Comparison of contours shapes

Figure 7a shows the water velocity distribution using porous metal baffles of varying thicknesses (2, 6, 10, 14, and 18 mm) at a

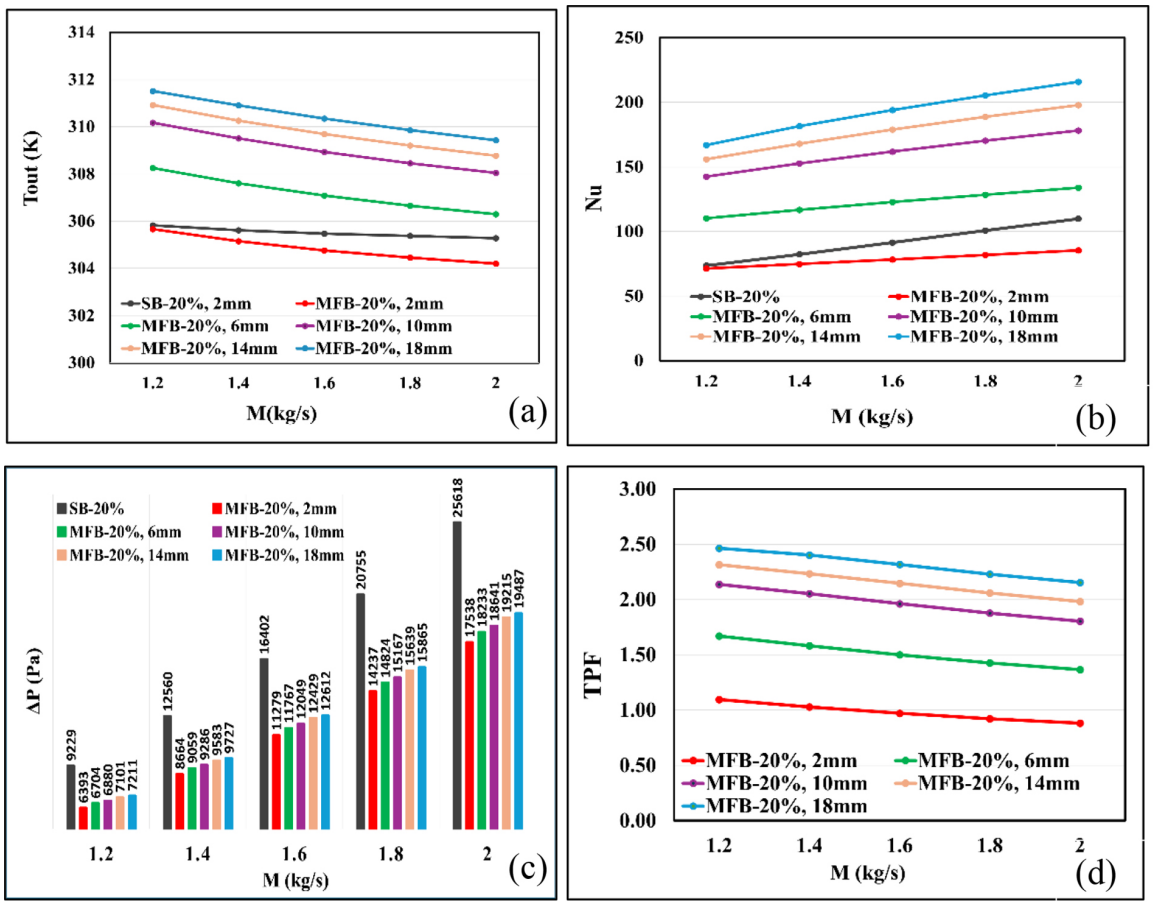

Figure 6. Outlet water temperature, Nu, pressure drop and TPF of STHX at different thickness

constant flow rate of 1.2 kg/s. Increasing the thickness diminishes the open area between the baffles, resulting in an increase in flow velocity and a reduction in the size of the low-velocity stagnation zones downstream of the baffles. Velocity vector distributions provide a physical interpretation of turbulence enhancement and flow restructuring induced by varying foam thickness. The results show that increasing foam thickness intensifies local recirculation zones and promotes deeper flow penetration within the porous baffle, leading to enhanced boundary-layer disruption and improved heat transfer, where increasing the thickness to 18 mm led to a 34% increase in Nu and 32% in TPF comparing with 6mm thickness. Simultaneously, the elongation of the effective flow path explains the observed trends in pressure drop.

Figure 7b illustrates that increasing the thickness of the MFB significantly improves the temperature distribution, resulting in more uniform thermal diffusion across the cross-sections. Foams with greater thicknesses (10–18 mm) exhibit a more uniform heat distribution, signifying enhanced efficiency in transferring thermal energy from the wall to the fluid. In thinner sections (2–6 mm), the temperature gradient remains pronounced due to the restricted surface area and inadequate transverse conductivity within the foam.

A comparison of contours in Figure 8 shows that small cut percentages (20%) enhance turbulence within the casing by generating vortices behind the baffles, increasing boundary layer regeneration and improving heat transfer efficiency, while keeping pressure drop within moderate levels due to some flow passing through the foam structure. Increasing the cut percentage reduces turbulence and leads to more uniform flow, thus decreasing heat exchange despite a lower ΔP. At 50%, bypass flow dominates, both turbulence and thermal performance decrease, while pressure drop reaches its minimum. Thus, optimal performance is achieved at a suitable balance between turbulence and hydraulic resistance, as seen at 20% BC.

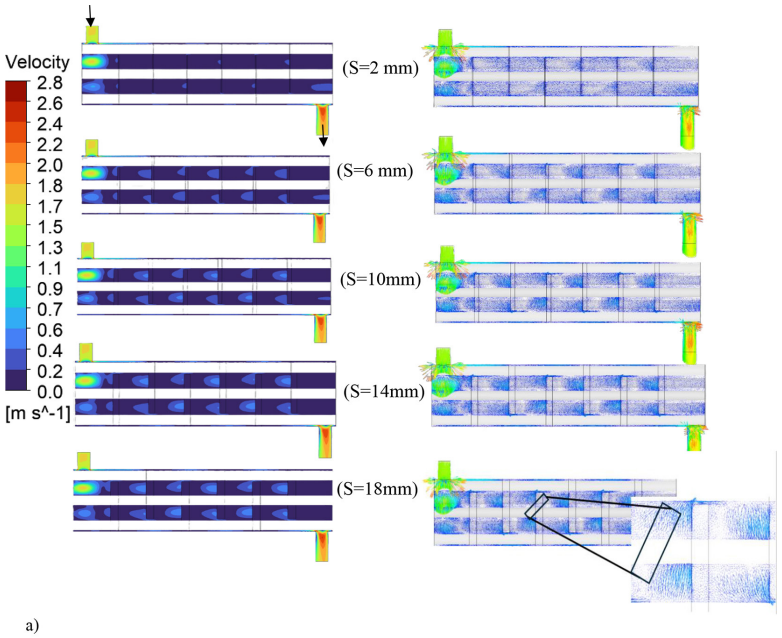

a)

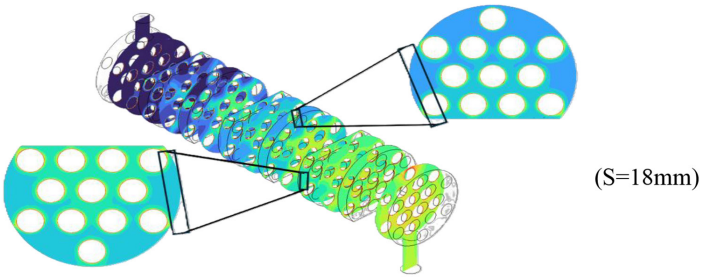

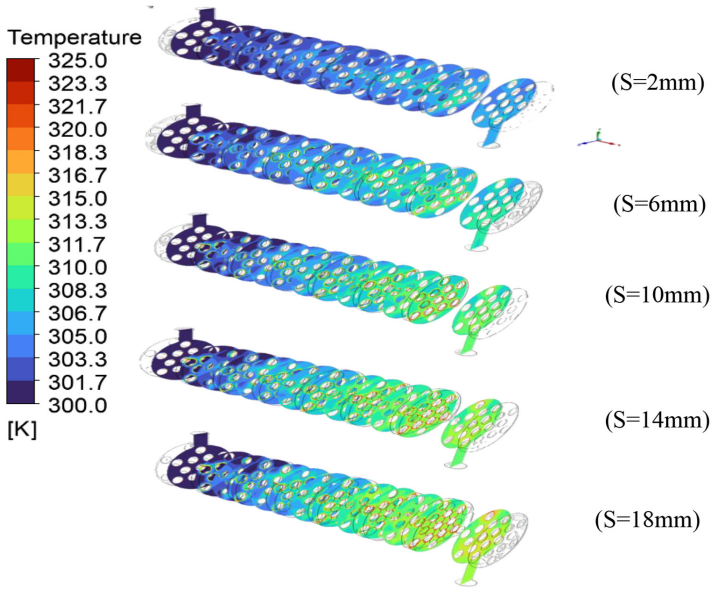

b)

Figure 7. a) Velocity contours and vectors of STHX at M= 1.2 kg/s with foam baffles with different thicknesses, b) Temperature contours of STHX at M= 1.2 kg/s with foam baffles with different thicknesses

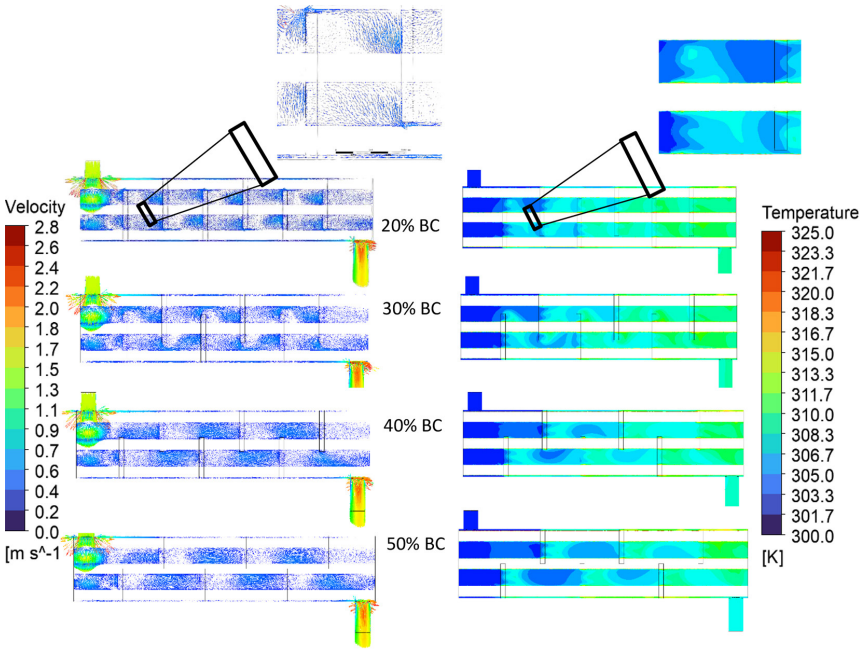

Figure 8. Velocity vectors and water temperature distributions at 1.2 kg/s for STHX equipped with foam baffles of different baffle cut ratio (Bcs)

Table 2. Correlation model's parameters

a_o	a_1	a_2	a_3	a_4	$\% \, error = \frac{\lvert TPF_{exp} - TPF_p \rvert}{TPF_{exp}}$
1.2142	0.0104	0.22	-0.2648	0.4497	2.45

Note: TPF_{exp}, TPF_p are the experimental and predicted values of TPF respectively. It can be seen that the model has excellent performance with absolute percentage error less than 3%. It is worth mentioning that the cross validation of four folds was utilized during the training and testing process.

Correlation equation of TPF

In the present study, the formula correlating the TPF values to Reynold's number (Re), Pressure drop (ΔP), Nusselt's number (Nu), and baffle thickness (S). A nonlinear formula was adopted for this correlation to account for the nonlinear relation between the dependent and independents variables as in Equation 23.

$$TPF = a_o . Re^{a_1} . (1 + \Delta P)^{a_2} . \; Nu^{a_3} . S^{a_4} + \epsilon \tag{23}$$

The parameters a_0, a_1, a_2, a_3, and a_4 are the model parameters while $\in$ is the error term. The experimental data was divided into 70% training sample and 30% testing sample. The training sample was used to train the model to extract the nonlinear relationships between the dependent and independent variables and estimate the optimum model parameters using the Levenberg–Marquardt algorithm. The testing sample was used to estimate the model performance in predicting the TPF. Table 2 shows the optimum model parameters and the percentage error for the testing sample.

CONCLUSIONS

The thermal and hydraulic performance (TPF) of metal foam baffle models with varying geometric characteristics was compared to STHXs employing conventional solid baffles. The results showed that using metal foam baffles simultaneously reduces pressure drop and increases the temperature difference between the water inlet and outlet, making them a more efficient option for this type of heat exchanger application. The key findings can be summarised as follows:

1. The outlet water temperature decreases with increasing baffle cut ratio (BC), due to the reduced heat exchange area and reduced turbulence in the shell side. Furthermore, increasing the water flow rate resulted in an additional temperature decrease, as this reduced the water's residence time within the system.
2. The 2 mm thickness exhibited poor thermal performance due the small effective heat exchange depth and heat transfer area. Meanwhile, increasing the mass flow rate also resulted in a lower outlet temperature due to the shorter residence time. Conversely, increasing the thickness improved heat transfer, with the greatest improvement of 48.57% at 18 mm thickness and 1.2 kg/s flowrate.
3. The study showed that using metallic foam as a baffle reduces pressure drop by 28.8% and 27% at flow rates of 2 and 1.2 kg/s, respectively, at a thickness of 6 mm compared to solid baffles, due to the high permeability of the foam that allows the fluid to pass through and reduces hydraulic resistance.
4. The pressure drops decreases as the (Bc) increases, due to the reduction in overall resistance of the flow. While it increases with growing flow rate as a result to the higher friction and turbulent flow. Also, it increases with increasing baffle thickness, due to the reduced open area and the longer flow path.
5. When varying the (Bc), the Nusselt number (Nu) showed the highest improvement with the Bc-20%, of 48.4%, at a M=1.2 kg/s due to enhanced turbulence. Regarding thickness, thicker baffles (18 mm) achieved an even greater improvement of 56%, compared to only 33.3% for thin baffles (6 mm) at the same flow rate.
6. Among the cases studied, STHX equipped with MF exhibited superior thermal and hydraulic performance compared to those with solid baffles, particularly at a thickness 18, 14.and 10 mm and a mass flow rate of 1.2 kg/s, with thermal performance factors (TPF) of 2.465,2.315 and 2.138 respectively. This optimized foam baffle design also resulted in a reduction in pressure loss of 21.8%, 23%, and 25.5%, confirming its effectiveness in simultaneously improving heat transfer and reducing hydraulic resistance.
7. An empirical nonlinear correlation was developed to correlate the TPF to the (Re, ΔP, Nu and S). The correlation model shows a high ability to estimate the TPF values with an averaged absolute error percentage less than 3%.

REFERENCES

1. Schab R., Kutschabsky A., Unz S., Beckmann M., Numerical investigation of tubeside maldistribution in shell-and-tube heat exchangers, Heat Mass Transf. und Stoffuebertragung, 2024; 60(5): 851–859, https://doi.org/10.1007/s00231-023-03385-5
2. Marzouk S. A., Abou Al-Sood M. M., El-Said E. M. S., Younes M. M., and El-Fakharany M. K., A comprehensive review of methods of heat transfer enhancement in shell and tube heat exchangers, vol. 148, no. 15. Springer International Publishing, 2023. https://doi.org/10.1007/s10973-023-12265-3
3. Maghsoudali Y., Rastegarkoutenaei A., Sahami M., and Bandpy M. G., Investigation of the effect of using the finned tubes on the performance of shell and tube heat exchanger by 3D modeling, J. Energy Storage, vol. 56, no. October, 2022; 106031, https://doi.org/10.1016/j.est.2022.106031
4. García-Moreno F., Commercial applications of metal foams: Their properties and production, Materials (Basel)., 2016; 9(2): 20–24, https://doi.org/10.3390/ma9020085
5. Hossein M., Zamani M., Hoseinzadeh S., Application of porous-embedded shell and tube heat exchangers for the waste heat recovery systems, Applied Thermal Engineering 2022; 211: 118452.
6. Kiwan S., Alwan H., and Abdelal N., An experimental investigation of the natural convection heat transfer from a vertical cylinder using porous fins, Appl. Therm. Eng., 2020; 179: 115673, https://doi.org/10.1016/j.applthermaleng.2020.115673
7. Rong F., Shi B., and Cui X., Lattice Boltzmann simulation of heat and fluid flow in 3D cylindrical heat exchanger with porous blocks, Appl. Math. Comput., 2016; 276: 367–378, https://doi.org/10.1016/j.amc.2015.10.076
8. Chen T., Shu G., Tian H., Zhao T., Zhang H., and Zhang Z., Performance evaluation of metal-foam baffle exhaust heat exchanger for waste heat recovery, Appl. Energy, 2020; 266: 114875, https://doi.org/10.1016/j.apenergy.2020.114875
9. Alhusseny A., Turan A., and Nasser A., Rotating metal foam structures for performance enhancement of double-pipe heat exchangers, Int. J. Heat Mass Transf., 2017; 105: 124–139, https://doi.org/10.1016/j.ijheatmasstransfer.2016.09.055
10. Hu H., Lai Z., and Ding G., Heat transfer and pressure drop characteristics of wet air flow in metal foam with hydrophobic coating under dehumidifying conditions, Appl. Therm. Eng., 2018; 132: 651–664, https://doi.org/10.1016/j.applthermaleng.2018.01.010

11. Dongellini M., Naldi C., Cancellara S., and Morini G. L., Experimental measurements of thermal–hydraulic performance of aluminum-foam water-to-air heat exchangers for a HVAC application, Appl. Therm. Eng., 2022; 213: 118716, https://doi.org/10.1016/j.applthermaleng.2022.118716
12. Yang X., Xu F., Wang X., Guo J., and Li M. J., Solidification in a shell-and-tube thermal energy storage unit filled with longitude fins and metal foam: A numerical study, Energy Built Environ., 2023; 4(1): 64–73, https://doi.org/10.1016/j.enbenv.2021.08.002
13. Tamkhade P. K., Lande R. D., Gurav R. B., and Lele M. M., Investigations on tube in tube metal foam heat exchanger, Mater. Today Proc., 2023; 72: 951–957, https://doi.org/10.1016/j.matpr.2022.09.097
14. Hassan A. M., Alwan A. A., and Hamzah H. K., Numerical study of fan coil heat exchanger with copper foam, Int. J. Fluid Mach. Syst., 2023; 16(1): 73–88, https://doi.org/10.5293/ijfms.2023.16.1.073
15. Tian H. et al., Assessment and optimization of exhaust gas heat exchanger with porous baffles and porous fins, Appl. Therm. Eng., 2020; 178: 115446, https://doi.org/10.1016/j.applthermaleng.2020.115446
16. Rabeeah Z. S., Jubear A. J., and Al-Bugharbee H. R., Studying the influence of using metal foam baffles on the performance of double-pipe heat exchanger, J. Therm. Eng., 2025; 11(1): 196–214, https://doi.org/10.14744/thermal.0000913
17. Jubear A. J., Numerical study of heat transfer on using metal foam and nanofluid in double pipe heat exchanger, no. August, 2025.
18. Jadhav P. H., Gnanasekaran N., and Mobedi M., Analysis of functionally graded metal foams for the accomplishment of heat transfer enhancement under partially filled condition in a heat exchanger, Energy, 2023; 263: 3–5, https://doi.org/10.1016/j.energy.2022.125691
19. Nie C., Chen Z., Liu X., Li H., Liu J., and Rao Z., Design of metal foam baffle to enhance the thermal-hydraulic performance of shell and tube heat exchanger, Int. Commun. Heat Mass Transf., 2024; 159: 108005, https://doi.org/10.1016/j.icheatmasstransfer.2024.108005
20. Faal Z. S., Thermal performance assessment of metal foam heat exchanger: a numerical and experimental study, 2024.
21. Lei Y., Li Y., Jing S., Song C., Lyu Y., and Wang F., Design and performance analysis of the novel shell-and-tube heat exchangers with louver baffles, Appl. Therm. Eng., 2017; 125, 870–879, https://doi.org/10.1016/j.applthermaleng.2017.07.081
22. Bahiraei M., Naseri M., and Monavari A., Thermal-hydraulic performance of a nanofluid in a shell-and-tube heat exchanger equipped with new trapezoidal inclined baffles: Nanoparticle shape effect, Powder Technol., 2022; 395: 348–359, https://doi.org/10.1016/j.powtec.2021.09.009
23. Al-darraji A. R., Marzouk S. A., Aljabr A., Almehmadi F. A., Alqaed S., and Kaood A., Enhancement of heat transfer in a vertical shell and tube heat exchanger using air injection and new baffles: Experimental and numerical approach, Appl. Therm. Eng., 2024; 236: 121493, https://doi.org/10.1016/j.applthermaleng.2023.121493
24. Farhan T. H., Fadhil O. T., and Ahmed H. E., Performance of a double-pipe heat exchanger with different met-al foam arrangements, Anbar J. Eng. Sci., 2021; 12(2): 100–112, https://doi.org/10.37649/aengs.2021.171162
25. Jubear A. J., CFD Simulation of air flow through a copper foams fin heat sink under forced convection, Design Engineering 2022; no. March.
26. Tikadar A. and Kumar S., Local hotspot thermal management using metal foam integrated heat sink, Appl. Therm. Eng., 2023; 221: 119632, https://doi.org/10.1016/j.applthermaleng.2022.119632
27. Žkauskas A., Heat transfer from tubes in crossflow, Adv. Heat Transf., 1987; 18: 87–159, https://doi.org/10.1016/S0065-2717(08)70118-7
28. Wang D., Wang H., Xing J., and Wang Y., Investigation of the thermal-hydraulic characteristics in the shell side of heat exchanger with quatrefoil perforated plate, Int. J. Therm. Sci., 2021; 159: 106580, https://doi.org/10.1016/j.ijthermalsci.2020.106580
29. Liu H. et al., Constructal design of double-layer asymmetric flower baffles, Energy, 2023; 280: 430205, https://doi.org/10.1016/j.energy.2023.128254